Reproducibility of color measurement in an artificial plaque model

When analyzing color in vivo, there are also variables affecting the perception of color, such as variability between each angioscope and white balancing [9]. Therefore, to test for such variables in each "plaque", imaging was performed five times using a different angioscope with white balancing each time. The images were acquired from a proximal to distal direction in the artery and perpendicularly in the control sample. A rectangular area within the "plaque" (each consisting of 600–700 pixels) was selected as a ROI from on-line images, and light intensity and the distance from the angioscope lens to the "plaque" were adjusted manually to obtain the optimal brightness L*. Because selected ROIs could still have pixels without optimal L* values, such pixels were excluded, and the obtained b* values were analyzed for their distribution and were compared with those from the control sample.

The remaining porcine carotid artery was used to examine possible differences between images obtained in air and in injected physiologic saline solution to simulate clinical practice. The same segment of the artery was observed under each circumstance with the same angioscope and white balancing, and a circular area corresponding to 600–700 pixels was selected as a ROI. Light intensity and the distance from the angioscope lens to the surface were fixed with optimal brightness L*. After the exclusion of pixels without optimal L* values, the obtained L* and b* values were compared.

Histologic study using quantitative colorimetry

To test the ability of quantitative colorimetry to detect LCTCs, we examined the surface color in human tissue samples of atherosclerotic plaques.

(a) Procedure

The distance from the angioscope lens and the angle of the angioscope to the sample were fixed at 3 mm and 45°, respectively. Images of the sample were acquired longitudinally. The vertical center of the circular angioscopic image was aligned to the reference of the scale at 3 mm intervals from the distal 1 mm of the proximal edge of the sample. Also, at each interval, 1–3 images were obtained horizontally in order to acquire the whole width of the sample. On an acquired on-line image, a rectangular area corresponding to 800–1,200 pixels out of the whole circular angioscopic image was selected as the ROI if it had homogeneous color visually. The vertical center of both the ROI and the whole circular angioscopic image were the same. At the ROI, intensity of light was adjusted manually to obtain adequate brightness L*, which was judged to be optimal when the mean value with SD of brightness L* was within the optimal range. Then, the pixels without optimal range were excluded from the selected ROI. The ROI setting and the measurement of the color were performed two times. Intra-observer agreement for b* values was $r = 0.994$ ($P < 0.0001$). Then, the final obtained mean values of b* were expressed as the quantified color of each ROI in the blue–yellow axis.

(b) Histopathologic processing of tissue samples

After the image acquisition by angioscopy, the sample was snap-frozen in liquid nitrogen. At that time, the sample was fixed carefully on a piece of cucumber, as the transverse sections perpendicular to the long axis would be the cutting direction. Each sample was stored at –80°C, and then, was cut into 6-μm transverse sections at 3 mm longitudinal intervals, so that the crosscut images of the histopathology slices would correspond with the vertical center of the angioscopic ROI. Staining was performed with Hematoxylin-Eosin and Masson's trichrome. Eighty-eight histopathology slices corresponding to angioscopic ROIs could be collected. Based on the lesion classification by the American Heart Association [12], the single most predominant histopathologic feature for each slice was determined by the concordance of two specialists who were blinded to the angioscopic images, and categorized as follows: (1) Type 1 (initial lesion or preatheroma) = 10; (2) Type 2 (fibrous plaque or calcified plaque) = 43; (3) Type

3 (atheroma or fibroatheroma) = 30; (4) Type 4 (lesion with hemorrhage) = 5.

(c) Measurement of fibrous cap thickness

Images of histopathology slices were acquired by using the standard microscope and image software (Image-Pro Plus, version 4.1, Media Cybernetics, MD). Both angioscopy and histopathology images were composed by the image software (Adobe Photoshop 5.0) on the slide sheet (Microsoft Power Point X for Mac). Then, the location in the histopathology slice, identical with the angioscopic ROI, was identified by fitting the breadth of both angioscopy and histopathology images of the sample, and/or by the adjustment of the configuration. At the determined locations, if the lipid core underneath the fibrous cap could be identified, the fibrous cap thickness was measured at five different fibrous cap sites over the lipid core in 100× magnification images. The mean value of these five measurements was expressed as the fibrous cap thickness.

Statistical analysis

Continuous variables were presented as the mean value ±SD, or as the median value with 25th and 75th percentiles when appropriate. Correlation and group differences of continuous variables were assessed with Pearson's correlation coefficient, two-tailed *t*-test or Mann-Whitney *U*-test and *F* test for variance. A value of <0.05 was considered to indicate statistical significance.

Results

Optimal range of L*value to measure color

Brightness L* value was directly proportional to the degree of light intensity and inversely proportional to the distance from the scope to the sample [Fig. 1(a) and 1(b)], suggesting that the RGB values from the image acquisition system were appropriate for the calculation in the software program. b* value was approximately constant when L* value was within 40–80 [OR010: $b^* = 55.58 + 0.003L^*$, $r = 0.86$ ($n = 95$); CY010: $b^* = -32.88 + 0.004L^*$, $r = 0.82$ ($n = 100$); VI010: $b^* = -47.21 + 0.04L^*$, $r = 0.87$ ($n = 102$)] (Fig. 2). Within this optimal range of L*, there were significant differences in measured b* values between the three standard samples, as expected from their spectroradiometric characteristics (Table 1).

Adjustment of brightness L* for angle and POI

(a) Angle (Table 2)

With unadjusted L*, b* values at 90° and 60° were not significantly different ($P = 0.65$), however, b* values at 45° and 30° were significantly lower than that at 90° ($P < 0.0001$ for both). When L* value of the ROI was adjusted to within 40–80, there was no statistical difference in b* values between control at 90° and all other angles.

(b) POI

Brightness L* decreased from the center to the edge of the field of view, and b* values decreased towards the edge of the field of view when brightness L* was <40 [Fig. 3(b)]. However, adjusting L* value to within 40–80 (64.4 ± 7.09), resulted in a decrease in the variance of b* values [52.00 ± 9.65 before adjustment to 55.88 ± 3.48, $P = 0.03$ for the variance, Fig. 3(c)].

Reproducibility of color measurement in the yellow plaque model

For the ROI in each plaque model (Fig. 4), the mean percent of pixels excluded (L* outside 40–80), as well as the adjusted L* value, are shown on Table 3. b* values were not significantly different between the control and the five plaque models. In images in air and in saline solution, b* values were not significantly different for L* values within 40–80 (Table 3).

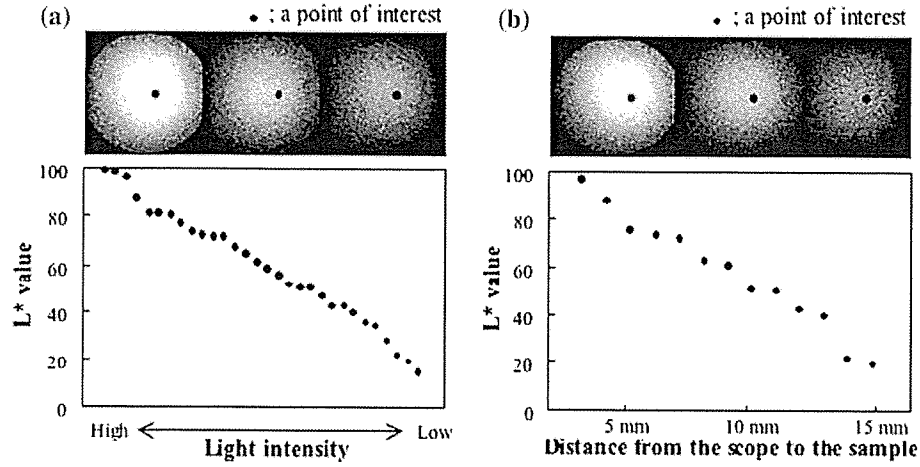

Fig. 1 Brightness L* value in relation to intensity of light (**a**) and distance from the angioscope to the sample (**b**). L* value was directly proportional to the degree of light intensity and inversely proportional to the distance from the scope to the sample

High yellow color intensity and LCTCs

Disruption or thrombus was not detected by histology in any of the samples (Fig. 5).

The median value of b* in each histopathology type was as follows: Type 1: –17.67 (–18.34 to –8.17); Type 2: –13.10 (–11.70 to –4.89); Type 3: 17.90 (10.44 to 18.83); Type 4: –24.39 (–25.16 to –22.06) (Fig. 6). The b* value of Type 3 was significantly higher than those of the other types ($P = 0.0002$ vs. Type 1; $P < 0.0001$ vs. Type 2 and Type 4, respectively). Among 43 Type 2 samples, nine calcified plaques had a clearly defined lipid core underneath a fibrous cap, and the b* value of these nine plaques [20.45 (14.35–26.29)] was not significantly different as compared with that of Type 3 ($P = 0.42$).

In the 38 samples with an identified lipid core underneath a fibrous cap (9 of 43 Type 2 and 29 of 30 Type 3), not including the Type 4 lesions (Fig. 7), b* value demonstrated an inverse linear correlation with the fibrous cap thickness (b* = 27.60–0.61 × fibrous cap thickness, $r = 0.51$, $P = 0.001$). In the 13 samples with a fibrous cap thickness <100 μm (10 fibroatheromas and three calcified plaques), the b* values were all ≥23 (35.91 ± 8.13).

In all Type 4 lesions, hemorrhage was detected in a lipid core by histopathology, and a visually dark blue appearance was seen in the ROIs of angioscopy (Fig. 5). The thickness of the fibrous cap was <100 μm (84.82 μm) in one of five samples, and >100 μm (175.22 ± 51.09 μm) in the remaining samples.

Discussion

We describe a quantitative colorimetric system based on the L*a*b* color space that could consistently measure atherosclerotic plaque color after proper adjustments for brightness. These adjustments are necessary because of changes in color perception that occur due to a number of variables unique to angioscopy, such as changes in light intensity, distance, and even the angle of the angioscope to the ROI. Our results revealed that the impact of these variables on color perception could be minimized by the brightness L* adjustment. In human atherosclerotic plaques, we found that high b* value (high yellow color intensity), determined by this quantitative colorimetric system, was associated with LCTCs.

Yellow plaque is thought to possess features commonly attributed to the atherosclerotic plaques vulnerable to thrombosis. Yellow color correlates with lipid-rich atheromas and thin fibrous caps [3, 4, 11]. Yellow coronary lesions have increased distensibility and are associated with compensatory outward remodeling [13],

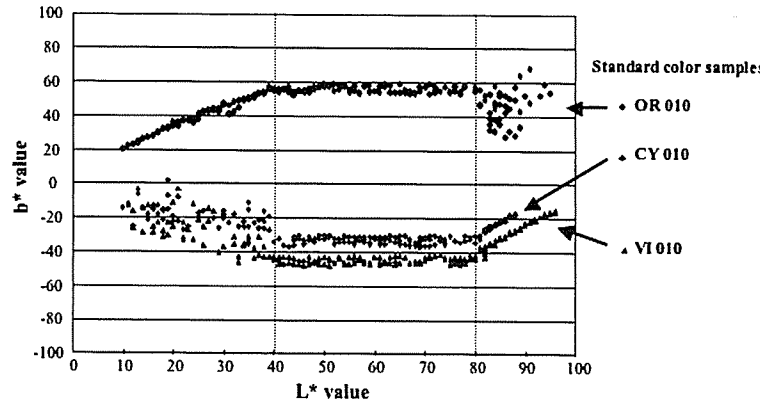

Fig. 2 In each of the three standard samples, b* value (yellow color intensity) was constant when L* was within 40–80

Table 1 Comparison of measured L*, b* values of standard color samples with quantitative colorimetry and actual values

Samples	Adjusted L* value	Measured b* value	Actual b* value
SCS-OR010	58.86 ± 11.70	55.73 ± 1.67**	43.74
SCS-CY010	61.21 ± 10.44	–32.63 ± 1.97**	–11.06
SCS-VI010	60.21 ± 12.32	–44.78 ± 1.69**	–22.77

Actual values are from spectroradiometry. **$P < 0.0001$; SCS-OR010 vs. CY010 or VI010; SCS-CY010 vs. VI010

Table 2 Comparison of b* values with non-adjusted or adjusted L* at various angles

Degree	L* value	b* value	*P* value for b* value vs. 90°
Non-adjusted			
90°	41.80 ± 20.92	34.64 ± 20.24	–
60°	30.64 ± 21.17	32.23 ± 19.30	0.65
45°	26.94 ± 20.60	28.96 ± 19.83	<0.0001
30°	22.28 ± 20.72	22.83 ± 19.05	<0.0001
Adjusted			
90°	68.89 ± 6.30	59.74 ± 8.56	–
60°	66.82 ± 6.01	60.56 ± 7.66	0.12
45°	63.54 ± 6.46	58.45 ± 8.11	0.11
30°	60.69 ± 6.90	57.18 ± 8.61	0.09

which may confer mechanical and structural weakness to the plaque. The plaque underlying coronary thrombus is usually yellow and/or disrupted as assessed by angioscopy [7], and these plaques are associated with higher frequency of adverse events after percutaneous coronary intervention [6], perhaps due to their thrombogenic nature. Multiple yellow plaques have been observed by angioscopy in non-culprit sites in patients with myocardial infarction [14], in support of the concept of pan-coronary vulnerability. Moreover, a clinical study demonstrated an association of yellow plaque with a higher incidence of future acute myocardial infarction [4], in which "glistening" yellow plaques were more likely to become future culprit lesions. Our previous study suggested that plaque color changes from yellow to white might indicate plaque stabilization by lipid-lowering therapy [15]. Thus, the body of evidence suggests that yellow color may be indicative of vulnerable coronary lesions. However, plaque color assessment has traditionally been made subjectively, which has become one of the Achilles' heels of angioscopy to study a possible association between yellow lesion and vulnerability. Our findings indicate that the quantitative colorimetric system based on the L*a*b* color space could be used to consistently measure the color of atherosclerotic plaques during angioscopy.

In the experimental conditions, measured color of the standard calibration samples differed from the actual values by spectroradiometry because of the following possible sources of error of the color signal: (1) the optic fibers; (2) the xenon lamplight; (3) the CCD camera; (4) white balancing without the equal energy white color standard (which is difficult to preserve and is expensive, thus not convenient for clinical use); and (5) the theoretical correction processes for the light

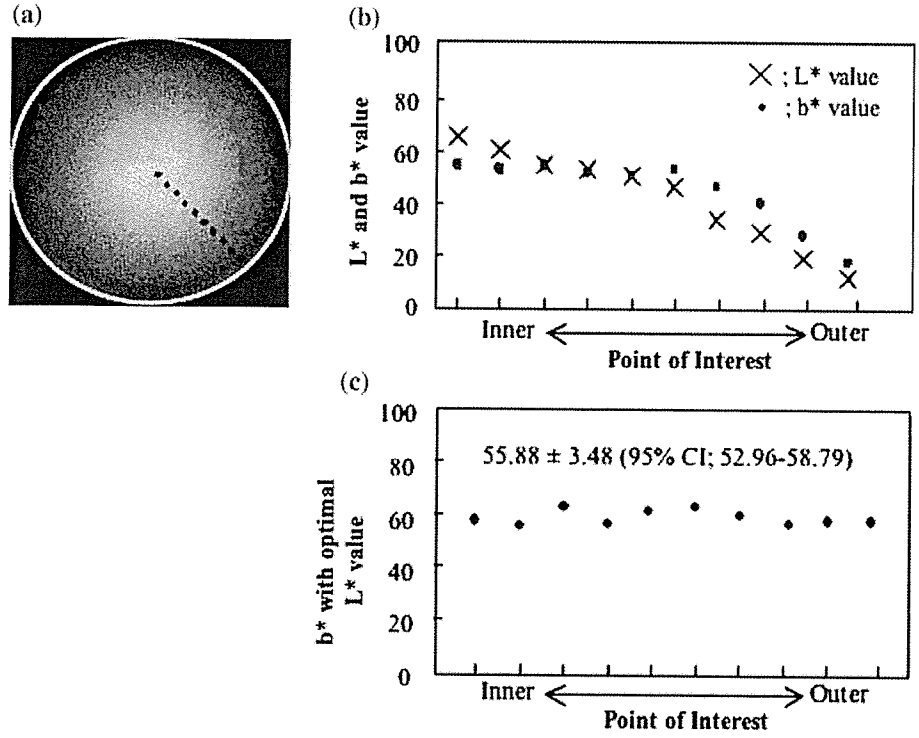

Fig. 3 (**a**) Displays 10 points of interest (POI) within the field of view from center to edge. (**b**) Unadjusted L* and b* values decreased from the center of the field of view to the edge. (**c**) After adjusting for L*, b* was similar among the different POI

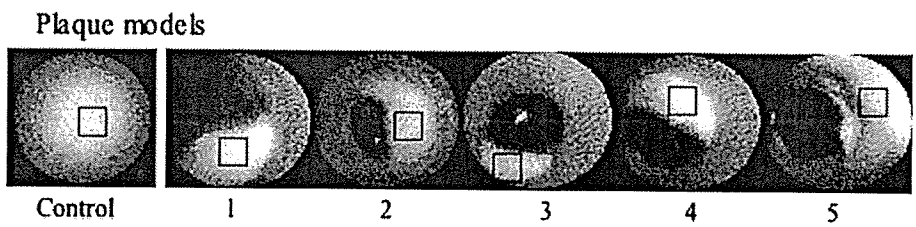

Fig. 4 Artificial yellow plaque models in porcine carotid arteries. A rectangular circle shows a region of interest

Table 3 Comparison of b* values with adjusted L* between various plaque models or between in air and in saline solution

	% Pixels excluded in ROI (L* outside 40–80)	Adjusted L* value	b* value	*P* value for b* value
Plaque models				*Versus Control*
Control	8.8	66.74 ± 8.02	67.54 ± 3.25	–
1	9.1	64.51 ± 8.54	66.07 ± 3.92	0.12
2	8.6	66.60 ± 8.35	67.76 ± 3.83	0.93
3	6.5	64.67 ± 8.30	66.04 ± 3.76	0.10
4	8.9	64.88 ± 9.39	66.18 ± 4.64	0.55
5	8.6	64.50 ± 10.23	65.18 ± 5.04	0.08
Air/Saline				*Versus air*
Air	6.8	58.50 ± 12.54	–7.27 ± 2.85	–
Saline solution	7.5	58.13 ± 11.32	–7.40 ± 2.68	0.66

ROI = region of interest

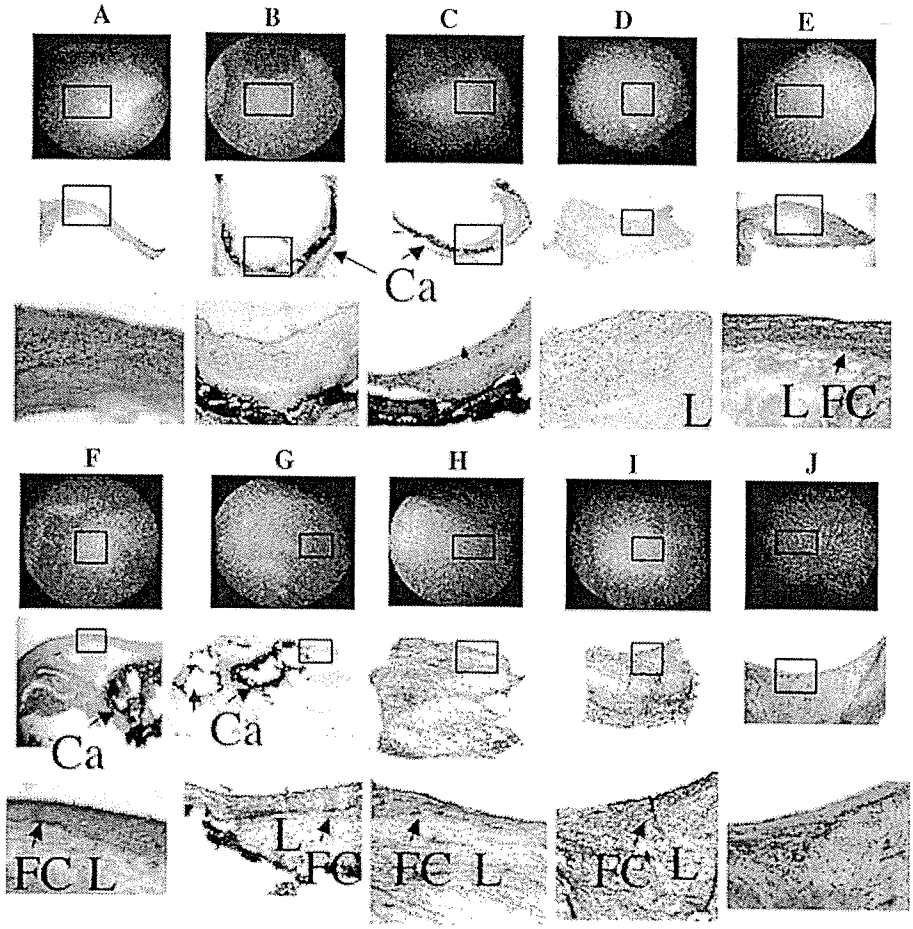

Fig. 5 Upper pictures show angioscopy images and the rectangular circles indicate the regions of interest (ROI). Middle pictures (H&E or Masson's trichrome stain, 12.5×) show the corresponding histology slices and the rectangular circles indicate the locations corresponding to the ROI of angioscopy images. Lower pictures (H&E or Masson's trichrome stain, 100×) show the larger view of the rectangular circles in the middle pictures. Ca = calcium, L = lipid core, FC = fibrous cap. (**A**) intimal lesion; (**B**) fibrous lesion; (**C**), (**F**), (**G**) calcified lesion; (**D**) atheroma; (**E**), (**H**), (**I**) fibroatheroma; (**J**) lesion with hemorrhage

temperature or the gamma value. It is complicated to quantify color completely using current angioscopic systems because of the multidimensional characteristics of color. However, in our study, we used the A/D converter and the computer software without the original color correction circuit. All images during white balancing were analyzed and L*, a* and b* values were 100, 0 and 0 in the whole field of view (data not shown), suggesting that each white balancing process was the same. By using L*a*b* color space, L* values were useful, as brightness was used to determine the optimal condition during the procedures of not only image acquisition but also of image analysis. In addition, the different color intensity of standard color samples could be measured through the same algorithm with minimum variances. Therefore, this system can be acceptable for consistent measurement of color during angioscopy, which is consistent with the study by Lehmann et al. [9, 10], and the quantified value can be compared between different atherosclerotic plaques.

Our findings indicate that high yellow color intensity, determined by b* values, could be used as a surrogate for the structural change of LCTCs in atherosclerotic plaques. The association of yellow color with a lipid core is consistent with prior

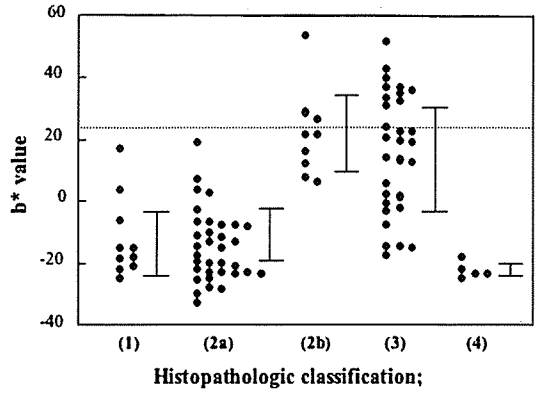

(1) Type 1=initial lesion, fatty streak and preatheroma (n=10).
(2a) Type 2 without lipid cores underneath fibrous caps (n=34).
(2b) Type 2 with lipid cores underneath fibrous caps (n=9).
(Type 2=fibrous and calcified plaque).
(3) Type 3=atheroma and fibroatheroma (n=30).
(4) Type 4=lesion with hemorrhage (n=5).

Fig. 6 b* value was higher in Type 3 (atheroma/fibroatheroma) lesions. Among 43 Type 2 (fibrous/calcified plaque) lesions, nine calcified plaques had lipid cores underneath fibrous caps, and yellow color intensity of these nine plaques was comparable with Type 3 [$P < 0.0001$ for (3) vs. (1) and (2), (2) vs. (4); $P = 0.0002$ for (1) vs. (4); $P < 0.0001$for (5) vs. (3) and (4)]

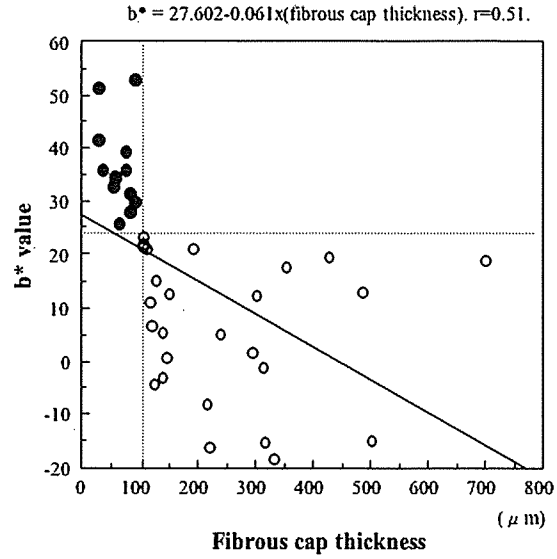

Tissue samples with identifiable lipid cores underneath thin fibrous caps (n = 38)

Fig. 7 Among 38 regions [9 Type 2 (fibrous/calcified plaque) and 29 Type 3 (atheroma/fibroatheroma) with identified lipid cores underneath fibrous caps], b* value demonstrated an inverse linear correlation with the fibrous cap thickness covering the lipid core. Yellow color intensity was high (b* ≥ 23: represented by black circles) in all locations with the fibrous cap thickness < 100 μm

angioscopy studies [3, 4]. However, the dispersion of yellow color among various types of plaque in our study suggests that surface yellow color may be determined not only by a lipid core but also by the various degrees of superficial intra- or extra-cellular lipids, consistent with histopathologic studies [12], because intimal cholesterol in human atherosclerotic plaques, in general, contains β-carotene that are yellow colored lipids [16]. The strong association between high yellow color intensity and LCTCs in our study is in line with the study by Miyamoto et al. [11], in which the percent saturation of yellow color increased inversely with the thickness of fibrous caps in fibroatheromas. Our results indicate that, once the fibrous cap above a lipid core becomes thinner than 100 μm, both the lipid core and the thin fibrous cap determine high yellow color intensity at such region. Our study also suggests that high yellow color intensity regions may be independent of the deeper segmental histopathology. Miyamoto et al. suggested that yellow color of the plaque surface reflects the presence of lipid pools up to 300 (m in depth [11]. Kawasaki et al. also demonstrated that visually assessed deep yellow color of coronary plaques was associated only with a thin fibrous cap above a lipid core, using both angioscopy and integrated backscatter analysis by intravascular ultrasound [17]. Thus, high yellow color intensity regions may not necessarily represent thin-cap fibroatheromas, the most common type of suspected vulnerable plaques based on histologic studies [18], but LCTC in a certain area of atherosclerotic plaques. This gives further support to the association of yellow plaque color with thrombus seen in clinical studies [3–8], because lipid cores are thrombogenic [19]. An exception would be lesions with severe intraplaque hemorrhage near the surface area, as LCTCs in these lesions did not appear yellow but bluish, perhaps because the surface color of tissue samples could change from red to violet by the deoxygenated blood component [20]. These lesions may have a reddish discoloration in vivo, as suggested by the study of Thieme et al. [3], in which a yellow–red plaque color was associated with atheroma or degenerated plaques with patchy necrosis. It is thus possible that red color appearance of plaque may also be useful to identify high-risk coronary sites.

A recent study indicated the possible link between intraplaque hemorrhage and plaque vulnerability prone to thrombosis [21], and yet another study suggested that angioscopy can be used to detect macrophage infiltration [22].

There are several limitations in the present study. First, we used three standard color samples with rather different b* values, which may limit the interpretation of the ability of our system to provide a precise discrimination between colors. However, the association between high yellow color intensity and LCTCs suggests that it may be acceptable for characterization of LCTCs as discussed above. Second, although the image acquisition of tissue samples was performed shortly after excision, changes in b* value must be considered because, if the blood component was rich near the surface area, the surface color may be expressed as a lower b* value (bluish hue) in tissue samples [20]. However, the fact that high b* values were measured in LCTCs suggests that this effect may not have a significant impact on the association of high b* value with LCTCs. Third, the materials of endarterectomy specimens in human atherosclerotic plaques of carotid or femoral arteries may limit the application of the association of high yellow color intensity with LCTCs to coronary arteries, and the number of specimens were relatively small, Further validation of high yellow color intensity regions will be required in ex-vivo and in-vivo human coronary arteries.

In the clinical setting, quantitative colorimetry during angioscopy could be useful to evaluate the possible relationship of LCTCs with plaque vulnerability by investigating their natural history. The clinical utility of angioscopy is limited to selected patients, since angioscopy as a routine imaging technique is impractical because of its invasive nature and the potential risk during the examination as displacement of blood is required [23]. Nevertheless, it can be useful as a research tool for vulnerable plaque and may guide novel diagnostic and therapeutic modalities in high-risk patients.

Conclusions

Atherosclerotic plaque color can be consistently measured with this quantitative colorimetric system based on the L*a*b* color space during angioscopy, if adjustments are made for brightness. High yellow color intensity, determined by this system, was associated with LCTCs. Therefore, angioscopy with quantitative colorimetry may be useful to detect LCTCs, which may be markers of vulnerable plaques.

Acknowledgements This study was supported in part by Research Grants from Fukuda Kinenn Foundation (to F.I) and for Cardiovascular Disease (15-5) from The Japanese Ministry of Health, Labor and Welfare (to K.M).

References

1. Falk E (2006) Pathogenesis of atherosclerosis. J Am Coll Cardiol 47:C7–C12
2. Waxman S, Ishibashi F, Muller JE (2006) Detection and treatment of vulnerable plaques and vulnerable patients: novel approaches to prevention of coronary events. Circulation 114:2390–2411
3. Thieme T, Wernecke KD, Meyer R et al (1996) Angioscopic evaluation of atherosclerotic plaques: validation by histomorphologic analysis and association with stable and unstable coronary syndromes. J Am Coll Cardiol 28:1–6
4. Uchida Y, Nakamura F, Tomaru T et al (1995) Prediction of acute coronary syndromes by percutaneous coronary angioscopy in patients with stable angina. Am Heart J 130:195–203
5. Mizuno K, Miyamoto A, Satomura K et al (1991) Angioscopic coronary macromorphology in patients with acute coronary disorders. Lancet 337:809–812
6. Waxman S, Sassower M, Mittleman M et al (1996) Angioscopic predictors of early adverse outcome following coronary angioplasty in patients with unstable angina and non-Q wave myocardial infarction. Circulation 93:2106–2113
7. Waxman S, Mittleman MA, Zarich SW et al (1997) Angioscopic assessment of coronary lesions underlying thrombus. Am J Cardiol 79:1106–1109
8. den Heijer PJ, Foley DP, Hillege HL et al (1994) The "Ermenonville" classification of observations at coronary angioscopy: evaluation of intra-and inter-observer agreement. European Working Group on Coronary Angioscopy. Eur Heart J 15:815–818
9. Lehmann KG, Oomen JA, Slager CJ et al (1998) Chromatic distortion during angioscopy: assessment and correction by quantitative colorimetric angioscopic analysis. Cathet Cardiovasc Diagn 45:191–201
10. Lehmann KG, van Suylen RJ, Stibbe J et al (1997) Composition of human thrombus assessed by quantitative colorimetric angioscopic analysis. Circulation 96:3030–3041
11. Miyamoto A, Prieto AR, Friedl SE et al (2004) Atheromatous plaque cap thickness can be determined by quantitative color analysis during

angioscopy: implications for identifying the vulnerable plaque. Clin Cardiol 27:9–15
12. Stary HC, Chandler AB, Dinsmore RE et al (1995) A definition of advanced types of atherosclerotic lesions and a histological classification of atherosclerosis. A report from the Committee on Vascular Lesions of the Council on Arteriosclerosis, American Heart Association. Circulation 92:1355–1374
13. Takano M, Mizuno K, Okamatsu K et al (2001) Mechanical and structural characteristics of vulnerable plaques: analysis by coronary angioscopy and intravascular ultrasound. J Am Coll Cardiol 38:99–104
14. Asakura M, Ueda Y, Yamaguchi O et al (2001) Extensive development of vulnerable plaques as a pan-coronary process in patients with myocardial infarction: an angioscopic study. J Am Coll Cardiol 37:1284–1288
15. Takano M, Mizuno K, Yokoyama S et al (2003) Changes in coronary plaque color and morphology by lipid-lowering therapy with atorvastatin: serial evaluation by coronary angioscopy. J Am Coll Cardiol 42:680–686
16. Blankenhorn DH, Freiman DG, Knowle HC (1956) Cartenoids in man: the distribution of epiphasic cartenoids in atherosclerotic lesions. J Clin Invest 35:1243–1247
17. Kawasaki M, Takatsu H, Noda T et al (2002) In vivo quantitative tissue characterization of human coronary arterial plaques by use of integrated backscatter intravascular ultrasound and comparison with angioscopic findings. Circulation 105:2487–2492
18. Virmani R, Kolodgie FD, Burke AP et al (2000) Lessons from sudden coronary death: a comprehensive morphological classification scheme for atherosclerotic lesions. Arterioscler Thromb Vasc Biol 20:1262–1275
19. Fernandez-Ortiz A, Badimon JJ, Falk E et al (1994) Characterization of the relative thrombogenicity of atherosclerotic plaque components: implications for consequences of plaque rupture. J Am Coll Cardiol 23:1562–1569
20. Kienle A, Lilge L, Vitkin IA et al (1996) Why do veins appear blue? A new look as an old question. Appl Optics 35:1151–1160
21. Kockx MK, Cromheeke KM, Knaapen MWM et al (2003) Phagocytosis and macrophage activation associated with hemorrhagic microvessels in human atherosclerosis. Arterioscler Thromb Vasc Biol 23:440–446
22. Kurita A, Ishizuka T, Matsui T et al (2004) Significance of angioscopic morphology for the estimation of macrophage infiltration and vascular physiology. Int J Cardiovasc Imag 20:165–171
23. Ishibashi F, Aziz K, Abela GS et al (2006) Update on coronary angioscopy: review of a 20-year experience and potential application for detection of vulnerable plaque. J Intervent Cardiol 19:17–25

European Heart Journal (2006) 27, 2189–2195
doi:10.1093/eurheartj/ehl181

Angioscopic differences in neointimal coverage and in persistence of thrombus between sirolimus-eluting stents and bare metal stents after a 6-month implantation

Masamichi Takano, Takayoshi Ohba, Shigenobu Inami, Koji Seimiya, Shunta Sakai, and Kyoichi Mizuno*

Department of Internal Medicine, Chiba-Hokusoh Hospital, Nippon Medical School 1715 Kamakari, Imba, Chiba 270-1694, Japan

Received 18 February 2006; revised 15 June 2006; accepted 14 July 2006; online publish-ahead-of-print 7 August 2006

See page 2147 for the editorial comment on this article (doi:10.1093/eurheartj/ehl170)

KEYWORDS
Stent;
Neointimal hyperplasia;
Thrombus

Aims The neointimal coverage and intracoronary thrombi within stented segments at 6 months after implantation between sirolimus-eluting stents (SESs) and bare metal stents (BMSs) were compared by direct visualization using angioscopy.

Methods and results Forty-six patients (36 stable angina and 10 acute coronary syndrome) were treated with 33 SESs and 33 BMSs. Immediately after and 6 months after stenting, each of the stented segments, edge body, and overlapping segment were observed by angioscopy and the grade of neointimal coverage over the stents was classified as 0: absent neointima, 1: visible struts through thin neointima, or 2: invisible struts. The existence of thrombi was also evaluated. The average grade of the neointimal coverage at 6 months follow-up was lower in the SES than that in the BMS (edge: 1.4 ± 0.7 vs. 1.9 ± 0.2, body: 1.0 ± 0.5 vs. 1.8 ± 0.5, overlapping segment: 0.6 ± 0.7 vs. 1.8 ± 0.5; $P < 0.0001$, $P < 0.0001$, $P = 0.0069$, respectively). The frequency of persistence of thrombus was significantly higher in the SESs than that in the BMSs (86 vs. 29%, respectively; $P = 0.031$).

Conclusion The present study suggested a delayed neointimal stent coverage and slower thrombus disappearance process in the SESs in comparison to the BMSs.

Introduction

To date, stent implantation has become the standard therapy in percutaneous coronary intervention (PCI) for patients with atherosclerotic coronary disease. Nevertheless, in-stent restenosis (ISR) within 3–8 months is a factor that limits the long-term success of stenting and it is mainly caused by neointimal hyperplasia.[1] Recently, sirolimus, a cytostatic macrocyclic lactone with both anti-inflammatory and antiproliferative properties, delivered from a polymer-encapsulated stent was shown in several angiographic and intravascular ultrasound (IVUS) studies to reduce the risk of ISR in comparison with the bare metal stent (BMS).[2–8] Neointimal proliferation inside the sirolimus-eluting stent (SES), which is recognized as lumen late loss on angiograms or as an obstruction volume on the IVUS, was minimal and nearly abolished at the 6-month follow-up.[4–7] Moreover, the in-stent lumen dimensions remained essentially unchanged for a long-term without a 'late catch-up'.[9] In contrast, there have been recent concerns regarding their potential for developing late-stent thrombosis related to the delayed re-endothelialization over the struts of the SES, particularly after discontinuation of dual antiplatelet therapy.[10,11] Therefore, it is important to know when complete re-endothelialization of drug-eluting stent occurs. If complete neointimal coverage of the drug-eluting stent is accomplished, thienopyridine may no longer be needed.

Coronary angioscopy provides a direct visualization of the luminal surface and detailed information on the state of stent coverage by the neointima, changes in the plaque colour, and the existence of intracoronary thrombi.[11–15] In this study, the condition of neointimal coverage and intracoronary thrombi over SESs are compared with those observed in BMSs at 6 months after their implantation.

Methods

Patients population

Between October 2004 and April 2005, 53 patients with *de novo* and native coronary artery lesions were treated with SESs (Cypher, Cordis Corp., Miami Lakes, FL, USA). During this study period,

* Corresponding author. Tel: +81 476 99 1111; fax: +81 476 99 1863.
E-mail address: mizunok@nms.ac.jp

© The European Society of Cardiology 2006. All rights reserved. For Permissions, please e-mail: journals.permissions@oxfordjournals.org

neither glycoprotein IIb/IIIa inhibitors nor clopidogrel had been approved for clinical use in Japan. Beforehand, all patients received two kinds of antiplatelet agents, ticlopidine 200 mg/day (standard dose under clinical approval in Japan) and aspirin 100–200 mg/day, longer than 48 h before the PCI for the prevention of acute or subacute thrombosis. Exclusion criteria were (i) acute myocardial infarction within 48 h from onset ($n = 3$), (ii) restenotic lesions after balloon angioplasty or ISR ($n = 7$), (iii) a low ejection fraction of the left ventricle ($n = 2$), (iv) left main disease or ostial lesions ($n = 12$), and (v) tortuous vessels or heavily calcified vessels proximal to the culprit lesions ($n = 8$) because of the expected difficulty in acquiring angioscopic images for the whole stented segments or in advancing the angioscopic catheter. Finally, 21 patients were enrolled in the SES group. Between October 2000 and May 2001, 61 patients were treated with BMSs. According to the above exclusion criteria, 36 patients (20 acute myocardial infarction, five restenosis, three low ejection fraction, four ostial lesions, and four vessel tortuousity or calcification) were excluded. Consequently, 25 patients were selected as the BMS group. All patients included this study received follow-up angiography and angioscopy at 6 months. Written informed consent approved by our institutional review board was obtained from all study patients before catheterization.

Clinical demographics

The patient demographics were obtained by a hospital chart review. Stable angina pectoris (SAP) was defined as a positive stress test and no change in the frequency, duration, or intensity of symptoms within 4 weeks. Unstable angina was new-onset severe angina, accelerated angina, or rest angina. Recent myocardial infarction was defined as its occurrence between 2 days and 2 weeks before the PCI. Patients with acute myocardial infarction less than 2 days from onset were not enrolled. Patients with unstable angina and recent myocardial infarction were categorized as acute coronary syndrome (ACS).

Culprit lesions (target lesions of the PCI) were identified by a combination of the ECG findings, wall motion abnormalities on left ventriculography or the echocardiography findings, and angiographic lesion morphology.

Angiographic analysis

All angiograms were analysed with a computer-assisted, automated edge detection algorithm (CMS, MEDIS, Nuenen, The Netherlands) by an angiographer blinded to the clinical and angioscopic findings using standard qualitative definition and quantitative coronary angiogram measurements. A 6-month follow-up angiogram was performed at the same angle as the PCI. The reference vessel diameter (RVD), minimal lumen diameter (MLD), per cent diameter stenosis (%DS), lesion length, and late loss at the culprit lesion or stented segment were measured. Angiographic filling defects, haziness, or wall irregularity was qualitatively evaluated. ISR was defined as more than or $\geq$50% of DS at follow-up, located within the stented segments and in the segments adjacent to the proximal and distal edge of the stent.

Coronary angioscopic imaging

The coronary angioscopic procedure has been previously reported.[12] Angioscopic examinations were performed before PCI, immediately after PCI, and 6 months after PCI as follow-up studies. Culprit plaques and whole-stented segments were observed with an angioscopic catheter (Vecmova Neo, Clinical Supply Corp., Gifu, Japan). The angioscopic images and fluoroscopy during the angioscopic observations were recorded on digital videotape for later analysis. The exact position of the angioscopic catheter at the observed segment was recorded by an angiogram to ensure a reliable comparison.

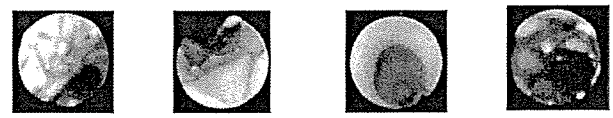

Figure 1 Angioscopic images of the neointimal stent coverage grade at follow-up and thrombus. (*A*) Stent coverage grade 0. No neointima was found on the struts of two overlapping SESs. The struts seemed to be completely exposed to the lumen. (*B*) Stent coverage grade 1. The struts were seen under the thin neointima. (*C*) Stent coverage grade 2. The struts were fully covered by white neointima and could not be seen. (*D*) Red thrombus was found around the struts (between 11 and 1 o'clock).

Definition and analysis of angioscopic findings

The plaque colour, the existence of a plaque rupture, and the existence of thrombus on the culprit plaque were evaluated before PCI. On the basis of the surface colour of the culprit plaque, the yellow grade was classified as 0 (white), 1 (light yellow), 2 (yellow), or 3 (dark yellow) according to the criteria established in our previous report.[13] A plaque rupture was defined as a complex plaque, which was considered to be present when the surface of the lesion had an irregular appearance, including a fissure, flap, and ulceration. A thrombus was defined a coalescent red or a pinkish-white, superficial or protruding mass adhering to the vessel surface but clearly a separate structure that remained, despite being flushed with a saline solution (*Figure 1*). Immediately after the PCI, both the plaque colour and the existence of thrombus within the stented segments were observed by repeat angioscopic examinations for a complete assessment of their angioscopic items. Six months after the PCI, the plaque colour, the existence of thrombus, and stent coverage by neointimal hyperplasia were all evaluated. The yellow grade regression was defined as the yellow grade immediately after stenting minus that at the 6-month follow-up. The extent of neointimal stent coverage was evaluated using a semi-quantitative grading system: 0, absent neointimal coverage by macroscopic detection; 1, visible struts through thin neointima; and 2, completely buried struts under the neointima (invisible struts through the neointima) (*Figure 1*). The neointimal stent coverage was estimated at major three different parts of the stented segment such as the edge the body, and the overlapping segment. Stent struts located at the orifice of the side branches were excluded from this evaluation. The minimum coverage grade at each segment was selected as the stent coverage grade.

The intra-observer agreement on angioscopic images was measured by having an observer repeat assessment of 20 images (presented in random order) after 1 week. The inter-observer agreement was measured by comparing the assessment of 50 images by the two observers blinded to the clinical background. The intra-observer agreements for the evaluated angioscopic items were 95% in existence of plaque rupture, 95% in yellow grade of the plaque, 100% in existence of thrombus, and 95% in stent coverage grade. The inter-observer agreements of those items were 92, 90, 96, and 90%, respectively.

Clinical follow-up

Two kinds of antiplatelet agents, ticlopidine (200 mg/day) added to aspirin (100–200 mg/day), were administered continuously during the 6-month follow-up period. Repeat PCI, coronary bypass surgery, the occurrence of ACS, and cardiac sudden death were all considered to be major adverse events.

Statistical analysis

The statistical analysis was performed using StatView 5.0 (SAS Institute). Categorical variables are presented as frequencies and

Table 1 Patients' characteristics

Patients	SES ($n=21$)	BMS ($n=25$)	P-value
Age (years)	66 ± 7	62 ± 11	0.12
Gender (male)	19 (90%)	20 (87%)	0.71
Coronary risk factors			
Diabetes mellitus	8 (38%)	6 (26%)	0.39
Hypertension	9 (43%)	12 (52%)	0.54
Hyperlipidaemia	14 (67%)	18 (78%)	0.39
Current smoking	8 (38%)	11 (48%)	0.52
Body mass index (kg/m^2)	24 ± 3	25 ± 4	0.36
Diagnosis of coronary artery disease			
SAP	16 (76%)	18 (78%)	0.87
ACS	5 (24%)	5 (22%)	
Prior myocardial infarction	9 (43%)	7 (30%)	0.39
Prior PCI	6 (29%)	5 (22%)	0.60
Prior bypass surgery	0 (0%)	0 (0%)	>0.99
Multi-vessel disease	10 (48%)	10 (43%)	0.78
Medications			
ACE-inhibitor or ARB	13 (62%)	12 (52%)	0.52
Beta-blocker	8 (38%)	12 (52%)	0.26
Calcium antagonist	5 (24%)	8 (35%)	0.43
Statin	17 (81%)	20 (87%)	0.59
Warfarin	1 (5%)	0 (0%)	0.48
Insulin	1 (5%)	1 (4%)	0.95
Oral hypoglycaemic agents	6 (29%)	5 (22%)	0.60

Values are n (%) or the mean ± SD. ACE, angiotensin-converting enzyme; ARB, angiotensin II receptor blocker.

they were analysed by either the χ^2 test or the Fisher's exact test. Continuous quantitative data and discontinuous data (angioscopic grades for plaque colour and stent coverage) are presented as mean ± SD. Continuous data were compared by the unpaired Student's t-test between the different categories. Ordinal data of stent coverage grade were tested by the Mann–Whitney U test with the Bonferroni's correction between the different categories (between different segments in the same kind of stent and corresponding segment between different kinds of stents). The yellow grade among the same categories between those observed at baseline and at follow-up was compared by the Wilcoxon singed-rank test with the Bonferroni's correction. A P-value of <0.05 was considered to be statistically significant.

Results

Clinical characteristics at baseline

Thirty-three SESs were implanted in 21 lesions of 21 patients and 33 BMSs were implanted in 28 lesions of 25 patients. The patients' characteristics in the SES group ($n=21$) and those in the BMS group ($n=25$) at baseline are summarized in *Table 1*. No significant difference in the age, proportion of gender, risk factors of atherosclerosis, including diabetes mellitus, diagnosis for coronary artery disease (SAP or ACS), or medications, existed between the two groups.

Angiographic findings

The angiographic data are summarized in *Table 2*. The lesion location did not differ between the two groups. Before PCI, RVD was greater in the BMS group than that in the SES group and the lesion length was longer in the SES group than that in the BMS group. The frequency of filling defects or haziness

Table 2 Angiographic findings

Patients	SES ($n=21$)	BMS ($n=25$)	P-value
Lesion location			
LAD	14 (67%)	17 (68%)	0.92
LCx	5 (24%)	4 (16%)	0.51
RCA	2 (9%)	7 (28%)	0.12
Before PCI			
RVD (mm)	2.81 ± 0.24	3.14 ± 0.32	0.0003
MLD (mm)	0.58 ± 0.31	0.59 ± 0.18	0.008
%DS	69.8 ± 13.8	71.0 ± 10.1	0.013
Lesion length (mm)	22.9 ± 10.8	13.0 ± 4.95	0.0002
Filling defects, haziness, or wall irregularity	4 (19%)	5 (20%)	0.94
Immediately after PCI			
MLD (mm)	2.64 ± 0.23	2.95 ± 0.25	0.00008
%DS	11.7 ± 2.97	12.8 ± 4.46	0.34
Acute gain (mm)	2.06 ± 0.32	2.36 ± 0.27	0.0013
Filling defects, haziness, or wall irregularity	2 (10%)	1 (4%)	0.45
Six-month follow-up			
MLD (mm)	2.55 ± 0.33	2.45 ± 0.65	0.53
%DS	14.0 ± 6.31	30.1 ± 15.1	0.00004
Late loss (mm)	0.09 ± 0.25	0.50 ± 0.57	0.0038
ISR	1 (5%)	6 (24%)	0.07
Filling defects, haziness, or wall irregularity	0 (0%)	0 (0%)	>0.99

Values are n (%) or the mean ± SD. LAD, left anterior descending artery; LCx, left circumflex artery; RCA, right coronary artery.

did not differ between the two groups. Immediately after PCI, both of MLD and acute gain were greater in the BMS group than that in the SES group. At the 6-month follow-up, both the %DS and late loss were smaller in the SES group than that in the BMS group. There were no filling defects, haziness, or wall irregularity in neither of the two groups at follow-up. Despite the fact that one case in the SES group showed focal ISR, no edge restenosis was seen on the angiogram. The SES group tended to show a decreased ISR rate in comparison to the SES group (5 vs. 24%, $P=0.07$).

Angioscopic findings

Angioscopic findings at baseline (before and immediately after PCI) and at the 6-month follow-up are summarized in *Table 3*. Before PCI, the frequency of plaque rupture and yellow grade of the culprit plaque did not differ between the two groups. At baseline, thrombus was observed in seven lesions (five in ACS and two in SAP) of seven SES patients and in seven lesions of seven BMS patients (five in ACS and two in SAP), and the frequency of the thrombus was similar between the two groups (33 vs. 28%, respectively). At the 6-month follow-up, the yellow grade of the culprit plaque was higher in the SES group than that in the BMS group (1.1 ± 0.5 vs. 0.5 ± 0.6, $P=0.0007$). The relatioship between the yellow grade regression and the frequency of the patients is presented in *Figure 2*.

Table 3 Angioscopic findings at baseline and follow-up

Patients	SES ($n = 21$)	BMS ($n = 25$)	*P*-value
Baseline			
Plaque rupture (Before PCI)	4 (19%)	5 (20%)	0.94
Yellow grade of the culprit plaque	1.4 ± 0.6	1.6 ± 0.9	0.39
Thrombus	7 (33%)	7 (28%)	0.022
Six-month follow-up			
Yellow grade of the culprit plaque	1.1 ± 0.5	0.5 ± 0.6	0.0007
Thrombus	7 (33%)	2 (8%)	0.049

Values are *n* (%) or mean ± SD.

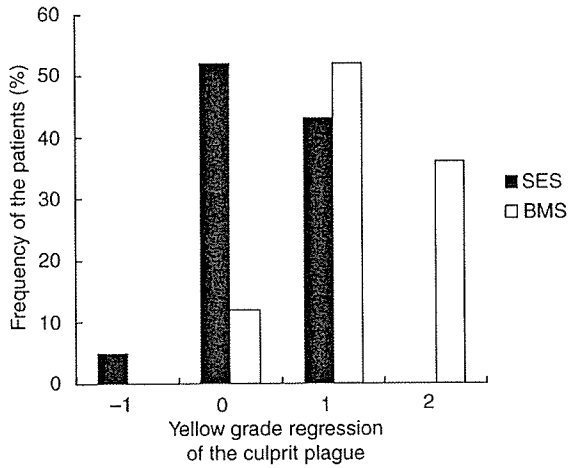

Figure 2 The relationship between the yellow grade regression of the culprit plaque and the frequency of the patients. In the SES group, the yellow grade regression of −1, 0, 1, and 2 were accounted for 5, 52, 43, and 0% of the patients, respectively. In the BMS group, that of −1, 0, 1, and 2 were accounted for 0, 12, 52, and 36% of the patients, respectively.

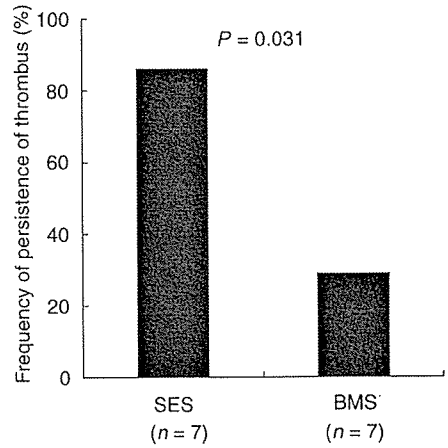

Figure 3 A comparison of the frequency of persistence of thrombus between the SES and BMS. The frequency of persistence of thrombus was significantly higher in the SES than in the BMS (86 vs. 29%, respectively).

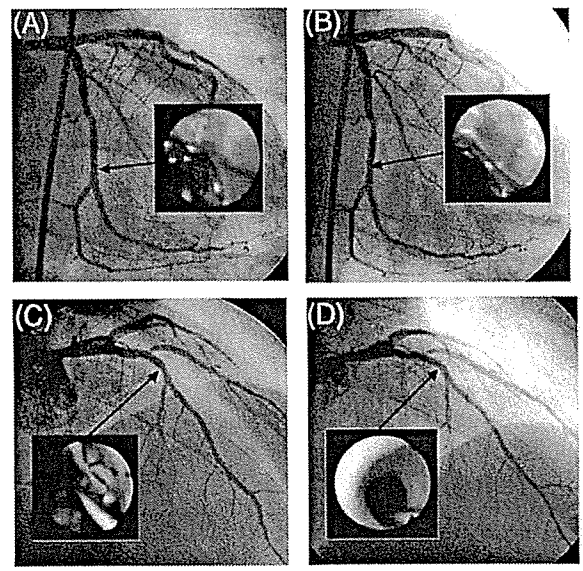

Figure 4 Two cases showing the angiographic and angioscopic findings after stent implantation in thrombotic lesions. (*A*) Immediately after SES implantation in the left circumflex artery in a patient with ACS. A pinkish mural thrombus was clearly found (between 0 and 5 o'clock) beside the plaque of the yellow grade 3 (at 11 o'clock). (*B*) A follow-up exam at 6 months in the case shown in (*A*). ISR was not seen on the angiogram. Residual thrombus was recognized (between 0 and 2 o'clock). Parts of the struts were absent in the neointimal coverage (the stent coverage grade 0), and a thin neointimal proliferation on the plaque of the yellow grade 2 (between 2 and 4 o'clock) was found. The yellow grade regression was 1 in this case. (*C*) Immediately after BMS implantation in the left anterior descending artery in a patient with ACS. A pinkish mural thrombus was found (between 0 and 8 o'clock) beside the plaque of the yellow grade 2 (between 0 and 3 o'clock). (*D*) A follow-up exam at 6 months in the case shown in (C). ISR was not seen on the angiogram. There was no residual thrombus. The struts were completely covered by neointima (the stent coverage grade 2 and the yellow grade 0). The yellow grade regression was 2 in this case.

The yellow grade regression of the culprit plaque was lower in the SES group than that in the BMS group (0.3 ± 0.6 vs. 1.1 ± 0.7, $P < 0.0001$). In the SES group, six of seven thrombi found at baseline remained at the 6-month follow-up, and one thrombus was newly recognized at follow-up. As a result, seven thrombi in the SES group were observed at follow-up. In the BMS group, two of seven thrombi found at baseline remained at the 6-month follow-up, and there was no thrombus formation during the 6-month follow-up period. The frequency of persistence of thrombus was higher in the SES group than that in the BMS group (86 vs. 29%, respectively; $P = 0.031$) (*Figure 3*). The angioscopic and angiographic findings for each case in the SES and the BMS groups are shown in *Figure 4*.

In the SES group, a single SES was deployed in 11 lesions, two SESs were placed in eight lesions, and three SESs were used in two lesions. In the BMS group, a single BMS was deployed in 23 lesions and two BMSs were placed in five lesions. In both of the groups, multiple stent deployment for a single lesion completely overlapped without a gap. At the 6-month follow-up, 21 stent edges, 33 stent bodies, and the 12 stent overlapping segments of the SES group were analysed for the stent coverage grade. Similarly, 28 stent edges, 33 stent bodies, and five stent overlapping segments of the BMS group were analysed. In all segments, the stent coverage grade for the SES was lower than that for the BMS (1.1 ± 0.7 vs. 1.9 ± 0.4, respectively; $P < 0.0001$).

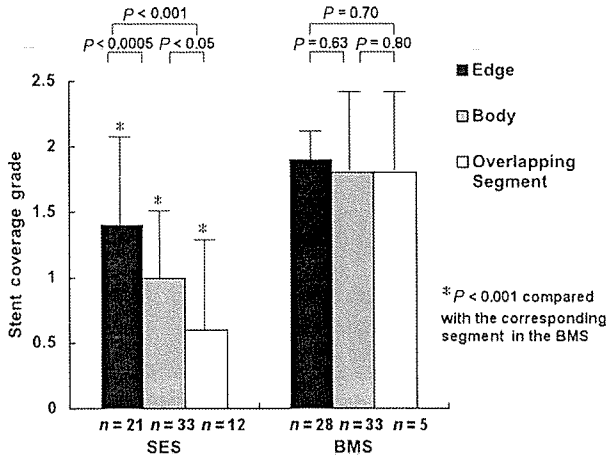

Figure 5 A comparison of the stent coverage grade in different stent segments between the SES and the BMS. The stent coverage grade in the SES was lower in the body than in the edge and in the overlapping segment than in the body. The coverage grade in the BMS did not differ between the edge, body, or the overlapping segment. This grade of the SES was lower than that of the BMS in every different segment.

The stent coverage grade in the SES was 1.4 ± 0.7 in edge, 1.0 ± 0.5 in body, and 0.6 ± 0.7 in overlapping segment. This grade was lower in the body than in the edge ($P = 0.0002$) and in the overlapping segment than in the body ($P = 0.016$). In the BMS group, the stent coverage grade in the edge body and overlapping segment was 1.9 ± 0.2, 1.8 ± 0.5, and 1.8 ± 0.5, respectively. No segment was significantly different from another. The stent coverage grade of the SES group was lower than that of the BMS group, in the edge ($P < 0.0001$), the body ($P < 0.0001$), and the overlapping segment ($P = 0.0069$) (*Figure 5*). A total of 27 segments (41% of all segments; six edges, 15 bodies, and six overlapping segments) of the SES and four segments (6% of all segments; four bodies) of the BMS were evaluated to have an absence of neointimal coverage (grade 0).

Clinical events

All patients underwent successful PCI for culprit lesions at baseline. Four lesions in three patients (12%) in the BMS group and none of the patients in the SES group underwent repeat PCI for ISR 6 months after the first PCI. All patients in both groups were free from bypass surgery, ACS, and cardiac sudden death during the clinical follow-up period.

Discussion

Although several follow-up studies after SES implantation revealed the effect of neointimal proliferation on its inhibition, there is a lack of detailed data regarding changes in underlying atherosclerotic yellow plaque due to neointimal stent coverage and intracoronary thrombus. Coronary angioscopy provides detailed information on plaque colour, neointimal hyperplasia, and mural thrombus by the direct visualization of the coronary lumen. Our angioscopic follow-up study demonstrated that the processes of changes in yellow plaque, neointimal coverage, and thrombus disappearance within the stented segments in the SES occurred more slowly than those in the BMS.

Differences in neointimal coverage between SES and BMS

The grade of neointimal coverage after BMS implantation was previously classified as either 0: complete exposure of stent struts, 1: exposure of the struts with partial coverage, 2: more than 50% coverage, 3: almost complete coverage with slightly visible the struts, or 4: complete coverage.[12] However, it was difficult to determine this grade from 1 to 3 after SES implantation, because neointimal growth over the SES was frequently too thin and was partially transparent. The transparent neointima diagnosed by angioscopy may be layer of fibrin deposition.[16] Therefore, simple grading system of the neointimal coverage was used in this study.

Experimental models of rabbit's iliac arteries confirmed that SES shows a decrease in neointimal thickness of 26.3% in comparison to BMSs (Bx velocity stents), platform of the SES.[16] At the 6-month follow-up, the late loss on the angiogram in the SES was smaller than that in the BMS. The stent coverage grade on the angioscopic findings in the overall stented segments in the SES was lower than that in the BMS. These results thus supported the notion that the neointimal proliferation inside the SES at the chronic phase was inhibited to be thinner than that in the BMS, and this finding was similar to the findings of previous IVUS investigations in living patients.[4,5,7,8]

One of the major factors that influence angioscopic yellow grade is thickness of the fibrous cap or neointima over atherosclerotic lipid contents. Thick neointimal hyperplasia after stenting might change the plaque colour from yellow to white or reduce the yellow grade. Therefore, the differences in the yellow grade regression of the culprit plaque between the SES and the BMS may be explained by the differences in the thickness of the neointimal hyperplasia. The thin neointima over the SES struts on the yellow plaque may make it easier to find the struts through the neointima and it may also be less influential in changing the yellow grade of the plaque.

Differences in neointimal coverage between the different segments

Angioscopic neointimal coverage over the BMS at the 6-month follow-up was almost complete and equal on the edge, in the body, and in the overlapping segment of the stents. In contrast, the degree of neointimal coverage of the SES differed between the edge, the body, and the overlapping segment. The neointimal coverage grade of the SES was significantly lower in the overlapping segment than in the body. These angioscopic results agree with the findings of a recent pathohistological report by Finn *et al.*[16] in which they demonstrated that both incomplete endothelialization (delayed endothelialization) as assessed by light microscopy and chronic inflammation were found more commonly in the overlapping segments than in the non-overlapping segments of the SES.[16] They speculated that the poor endothelialization and persistent inflammation in the overlapping segment are based on the contribution of drug overdose, a hypersensitive reaction to the polymer, and/or metal overload. In the present study, 27 of 66 segments (41%) of the SES were evaluated to have an absence of neointimal coverage and an exposure of the struts on angioscopy. A macroscopic diagnosis using

angioscopy has limitation to detect infiltration of inflammatory cells, tiny fibrin deposition, and very thin neointimal proliferation on the struts.[17] Other imaging modalities with a high-resolution, such as optical coherence tomography, may help to clarify the fine structure inside the SES.[17]

Previous IVUS studies revealed that the SES does not create any of the edge effects predominantly caused by negative remodelling with exaggerated neointimal hyperplasia.[5,7,8] In the present study, angioscopic neointimal coverage grade of the SES was higher in the edge than in the body at follow-up. The precise mechanism of the differences in the degree of neointimal proliferation is not clear. Several speculative hypotheses may be raised to explain this phenomenon. First, at the proximal or distal edges, the drug dose and/or metal dose of the SES is theoretically half of that in the body because the existence of the struts is only on one side, namely either the distal or the proximal side. Secondly, the edges of the SES are usually located in non-stenotic healthy segments, whereas its bodies are in the stenotic diseased segments on the angiogram. Therefore, the composition of the vessel wall (plaque) might differ between the two locations. These differences in the composition of vessel wall (plaque) may be the cause of the differences in the degree of neointimal proliferation on angioscopy.

Differences in thrombus disappearance between SES and BMS

After stent implantation, it has been understood that smooth muscle cells in the media proliferate and migrate to the lumen surface under the influence of growth factors.[18] However, the processes of thrombus disappearance after stenting in living patients are necessarily less detailed. The neointimal growth involved in the thrombus change to fewer cellular elements and a richer extracellular matrix probably occurs over a period of weeks or months.

In our series, the SES showed more unfavourable effects on the thrombus disappearance within the stented segments than the BMS. Several possible explanations can be offered for these results. First of all, sirolimus directly inhibits the proliferation of smooth muscle cells. As a result, thrombus disappearance may be indirectly delayed due to a suppression of neointimal growth. Secondly, the *in vitro* findings indicated that sirolimus (rapamycin) by itself increases basal tissue factor levels by 40% in human aortic endothelial cells.[19] The tissue factor, contained in human atherosclerotic plaques, is well known to be one of the thrombogenic agents. The tissue factor expressed on the endothelium may therefore disturb the thrombus disappearance.

Although angioscopy has limitations to confirm the existence of very thin neointima, macroscopic examinations at the 6-month follow-up failed to reveal a complete neointimal coverage overlying the struts, especially in the overlapping segment of the SES. Moreover, most of the intracoronary thrombi within the SES remained at follow-up. It may thus be necessary to investigate the duration of aggressive antiplatelet therapy after SES implantation. In the BMS, the phenomenon that the neointima becomes thick and non-transparent until 6 months after stent implantation and then thin and transparent by 3 years has been previously reported.[20] Further long-term follow-up studies to elucidate changes in the neointima and the residual thrombi are thus required.

Study limitations

Our findings were based on observations in a relatively small number of patients and stented segments excluding acute myocardial infarction within 48 h from onset. Some selection bias is therefore inevitable. This study was not a randomized study. Therefore, the RVD before the PCI was larger in the BMS group than in the SES group. The patient characteristics between the two groups were well matched. However, under these conditions, the antiproliferative effects of the SES were demonstrated by angioscopy.

Conclusions

This study failed to prove complete neointimal coverage of SES 6 months after implantation, despite macroscopic diagnosis by angioscopy. Our angioscopic study suggested both a delayed neointimal proliferation and a slow process in thrombus disappearance in the SES in comparison with those in the BMS at 6 months after their implantation. Further long-term follow-up studies to clarify the serial changes of the neointima and thrombi inside the SES are thus called for.

Acknowledgement

This study was supported in part by the Eisai Corporation.

Conflict of interest: none declared.

References

1. Kornowski R, Hong MK, Tio FO, Bramwell O, Wu H, Leon MB. In-stent restenosis: contributions of inflammatory responses and arterial injury to neointimal hyperplasia. *J Am Coll Cardiol* 1998;**31**:224–230.
2. Marx SO, Marks AR. Bench to bedside: the development of rapamycin and its application to stent restenosis. *Circulation* 2001;**104**:852–855.
3. Suzuki T, Kopia G, Hayashi S, Bailey LR, Llanos G, Wilensky R, Klugherz BD, Papandreou G, Narayan P, Leon MB, Yeung AC, Tio F, Tsao PS, Falotico R, Carter AJ. Stent-based delivery of sirolimus reduces neointimal formation in a porcine coronary model. *Circulation* 2001;**104**:1188–1193.
4. Sousa JE, Costa MA, Abizaid A, Abizaid AS, Feres F, Pinto IM, Seixas AC, Staico R, Mattos LA, Sousa AG, Falotico R, Jaeger J, Popma JJ, Serruys PW. Lack of neointimal proliferation after implantation of sirolimus-coated stents in human coronary arteries: a quantitative coronary angiography and three-dimensional intravascular ultrasound study. *Circulation* 2001;**103**:192–195.
5. Rensing BJ, Vos J, Smits PC, Foley DP, van den Brand MJ, van den Gissen WJ, de Feijter PJ, Serruys PW. Coronary restenosis elimination with a sirolimus eluting stent: first European human experience with 6-month angiographic and intravascular ultrasonic follow-up. *Eur Heart J* 2001; **22**:2125–2130.
6. Morice MC, Serruys PW, Sousa JE, Fajadet J, Ban Hayashi E, Perin M, Colombo A, Schuler G, Barragan P, Guagliumi G, Molnar F, Falotico R, RAVEL Study Group. A randomized comparison of a sirolimus-eluting stent with a standard stent for coronary revascularization. *N Engl J Med* 2002;**346**:1773–1780.
7. Serruys PW, Degertekin M, Tanabe K, Abizaid A, Sousa JE, Colombo A, Guagliumi G, Wijns W, Lindeboom WK, Lighthart J, de Feyter PJ, Morice MC, RAVEL Study Group. Intravascular ultrasound findings in the multicenter, randomized, double-blind RAVEL (Randomized study with the sirolimus-eluting Velocity balloon-expandable stent in the treatment of patients with de novo native coronary artery Lesions) trial. *Circulation* 2002;**106**:798–803.

8. Degertekin M, Lemos PA, Lee CH, Tanabe K, Sousa JE, Abizaid A, Regar E, Sianos G, van der Giessen WJ, de Feyter PJ, Wuelfert E, Popma JJ, Serruys PW. Intravascular ultrasound evaluation after sirolimus eluting stent implantation for de novo and in-stent restenosis lesions. *Eur Heart J* 2004;**25**:32–38.
9. Sousa JE, Costa MA, Abizaid A, Feres F, Seixas AC, Tanajura LF, Mattos LA, Falotico R, Jaeger J, Popma JJ, Serruys PW. Four-year angiographic and intravascular ultrasound follow-up of patients treated with sirolimus-eluting stents. *Circulation* 2005;**111**:2326–2329.
10. McFadden EP, Stabile E, Regar E, Cheneau E, Ong AT, Kinnaird T, Suddath WO, Weissman NJ, Torguson R, Kent KM, Pichard AD, Satler LF, Waksman R, Serruys PW. Late thrombosis in drug-eluting coronary stents after discontinuation of antiplatelet therapy. *Lancet* 2004;**364**:1519–1521.
11. Takano M, Mizuno K. Late coronary thrombosis in a sirolimus-eluting stent due to the lack of neointimal coverage. *Eur Heart J* 2006;**27**:1133.
12. Sakai S, Mizuno K, Yokoyama S, Tanabe J, Shinada T, Seimiya K, Takano M, Ohba T, Tomimura M, Uemura R, Imaizumi T. Morphologic changes in infarct-related plaque after coronary stent placement: a serial angioscopy study. *J Am Coll Cardiol* 2003;**42**:1558–1565.
13. Takano M, Mizuno K, Yokoyama S, Seimiya K, Ishibashi F, Okamatsu K, Uemura R. Changes in coronary plaque color and morphology by lipid-lowering therapy with atorvastatin: serial evaluation by coronary angioscopy. *J Am Coll Cardiol* 2003;**42**:680–686.
14. Okamatsu K, Takano M, Sakai S, Ishibashi F, Uemura R, Takano T, Mizuno K. Elevated troponin T levels and lesion characteristics in non-ST-elevation acute coronary syndromes. *Circulation* 2004;**109**:465–470.
15. Takano M, Inami S, Ishibashi F, Okamatsu K, Seimiya K, Ohba T, Sakai S, Mizuno K. Angioscopic follow-up study of coronary ruptured plaques in nonculprit lesions. *J Am Coll Cardiol* 2005;**45**:652–658.
16. Finn AV, Kolodgie FD, Harnek J, Guerrero LJ, Acampado E, Tefera K, Skorija K, Weber DK, Gold HK, Virmani R. Differential response of delayed healing and persistent inflammation at sites of overlapping sirolimus- or paclitaxel-eluting stents. *Circulation* 2005;**112**:270–278.
17. Takano M, Jang IK, Mizuno K. Neointimal proliferation around malapposed struts of a sirolimus-eluting stent: optical coherence tomography findings. *Eur Heart J* 2006;**27**:1763.
18. Welt FGP, Rogers C. Inflammation in the stent era. *Atheroscler Thromb Vasc Biol* 2002;**22**:1769–1776.
19. Steffel J, Latini RA, Akhmedov A, Zimmermann D, Zimmerling P, Luscher TF, Tanner FC. Rapamycin, but not FK-506, increases endothelial tissue factor expression. *Circulation* 2005;**112**:2002–2011.
20. Asakura M, Ueda Y, Nanto S, Hirayama A, Adachi T, Kitakaze M, Hori M, Kodama K. Remodeling of in-stent neointima, which become thinner and transparent over 3 years: serial angiographic and angioscopic follow-up. *Circulation* 1998;**97**:2003–2006.

Clinical vignette

doi:10.1093/eurheartj/ehi789

Huge right coronary artery aneurysm in a young adult

Kuan-Ming Chiu[1], Tzu-Yu Lin[2], and Ming-Jiuh Wang[3]*

[1]Department of Cardiovascular Surgery, Far Eastern Memorial Hospital, 21, Sec. 2, Nan-Ya South Road, Pan Chiao, Taipei 220, Taiwan; [2]Department of Anesthesia, Far Eastern Memorial Hospital, 21, Sec. 2, Nan-Ya South Road, Pan Chiao, Taipei 220, Taiwan; [3]Department of Anesthesiology, National Taiwan University Hospital and National Taiwan University College of Medicine, 7, Chung Shan South Road, Taipei 100, Taiwan

* Corresponding author. Tel: +886 2 23562010; fax: +886 2 23217522. *E-mail address*: canon@ha.mc.ntu.edu.tw

A 34-year-old man visited our institution for an abnormal chest radiograph with greatly enlarged cardiac silhouette (Panel A) found before his wedding. Detailed medical history revealed a febrile episode and a strawberry-like tongue and some 'flu-like symptoms' for >1 week when he was 5 years old. Diagnostic workup including computerized tomography demonstrated a huge right coronary artery aneurysm (Panel B). Intra-operative transesophageal echocardiography showed a large orifice of right coronary artery with a huge aneurysm (Panel C). The right coronary artery aneurysm was resected (Panel D) under hypothermic cardiopulmonary bypass with cardioplegic arrest. The diameter of the orifice of the right coronary artery was >20 mm, which was closed with Dacron patch, and the saphenous vein was used to bypass the right coronary artery to its two major branches. The patient had an uneventful recovery and was discharged 6 days after the operation.

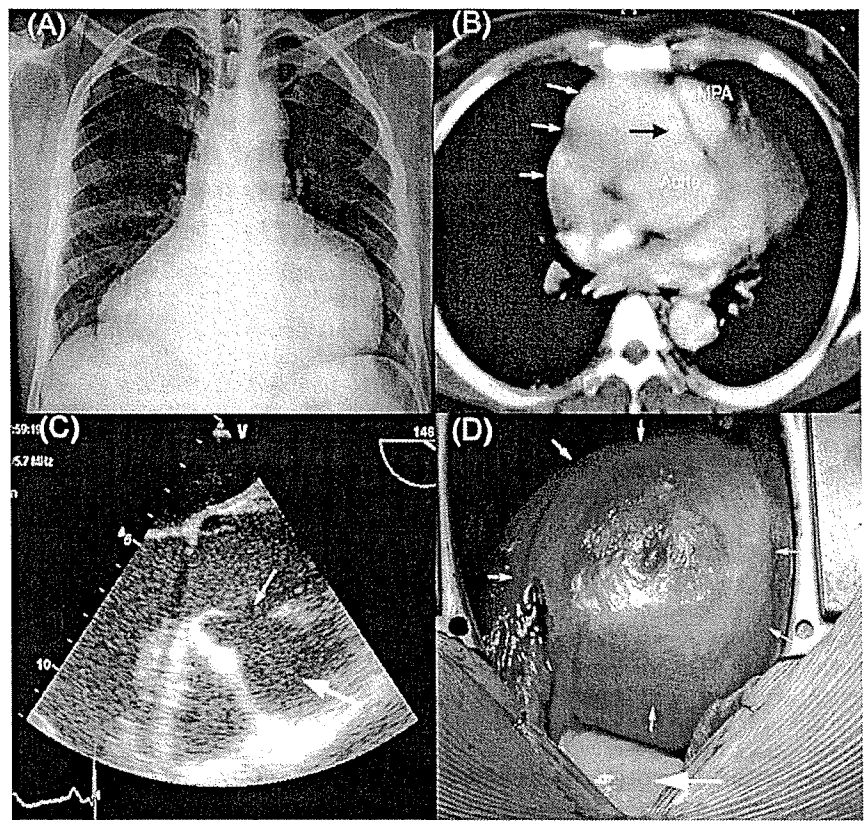

Panel A. Chest X-ray shows an enlarged cardiac silhouette.

Panel B. Thorax CT-scan shows the right coronary artery aneurysm (white arrows) and its connection (black arrow) with the aorta. MPA, main pulmonary artery.

Panel C. Transesophageal echocardiography shows the enlarged orifice of right coronary artery (small arrow) and the large aneurysm (large arrow).

Panel D. Surgical views of the huge right coronary artery aneurysm (small arrows) and aorta (large arrow).

—Report on Experiments and Clinical Cases—

Significance of Plaque Disruption Sites in Acute Coronary Syndrome

Koji Seimiya, Shigenobu Inami, Masamichi Takano, Takayoshi Ohba, Shunta Sakai, Teruo Takano and Kyoichi Mizuno

Cardiovascular Center, Chiba-Hokusoh Hospital, Nippon Medical School

Abstract

Coronary plaque disruption and subsequent thrombosis occur in both unstable angina (UA) and acute myocardial infarction (AMI). However, it is unclear why UA and AMI have different clinical courses. The purpose of this angiographic study was to examine whether the longitudinal plaque disruption site is a factor that can be used to distinguish these two conditions. Seventy-two patients with AMI or UA in whom ischemia- or infarct-related arteries and plaque disruption sites could be determined were enrolled. The plaque disruption sites were classified as upstream type or downstream type. The upstream type and downstream type were defined as plaque rupture site located proximal and distal, respectively, to the maximum stenosis on angiography. The frequency of the upstream type was significantly higher in patients with AMI (60.0%) than in patients with UA (18.5%). On the other hand, the frequency of the downstream type was higher in patients with UA (81.5%) in patients with AMI (40.0%; $p<0.01$). The longitudinal plaque disruption site may thus be a factor that can be used to distinguish these two diseases.

(J Nippon Med Sch 2006; 73: 141–148)

Key words: acute coronary syndrome, myocardial infarction, unstable angina, plaque disruption

Introduction

Coronary plaque disruption followed by thrombus formation is considered an important factor in the pathogenesis of acute coronary syndrome (ACS), including acute myocardial infarction (AMI) and unstable angina (UA), and results in progression of coronary stenosis, which can be confirmed with several kinds of studies such as pathologic examination, angiography, intravascular ultrasonography, and angioscopy[1–4]. Plaque disruption occurs mainly at so-called shoulder lesions showing focal accumulation of foam cells, a thin fibrous cap, and/or a large lipid pool and high circumferential stress on the plaque[4,5].

Although the depth of plaque disruption, the condition of the thrombus, and an interruption of blood flow may help differentiate AMI from UA[3], it remains unclear why these two clinical conditions arise from similar pathological conditions. The aim of this study was to identify an additional factor that can be used to distinguish AMI from UA. The basic principle at issue in this study is that the plaque disruption site may influence the clinical presentation of ACS. There is a possibility that

Correspondence to Kyoichi Mizuno, MD, Cardiovascular Center, Chiba-Hokusoh Hospital, Nippon Medical School, 1715 Kamakari, Inba-mura, Inba-gun, Chiba 270–1694, Japan
E-mail: mizunok@nms.ac.jp
Journal Website (http://www.nms.ac.jp/jnms/)

plaque rupture at a proximal site of plaque and thrombus formation might strongly interfere with the regulation of blood flow, in comparison to a plaque rupture at a distal site. We hypothesized that thrombus accompanied by plaque rupture at a proximal site might cause total occlusion and thus result in AMI. On the other hand, thrombus accompanied by plaque rupture at a distal site might induce nontotal occlusion and result in UA. To verify this hypothesis, we investigated plaque rupture sites in patients with ACS using coronary angiography.

Methods

We evaluated 348 consecutive patients who underwent coronary angiography and were diagnosed with AMI or UA from May 1997 through March 2004 at our institution. Patients in whom ischemia- or infarct-related arteries (IRAs) and plaque rupture sites could not be determined with angiography were excluded. Finally, 72 patients in whom IRAs and plaque rupture sites could be clearly determined with angiography were enrolled. Then we evaluated the locations of plaque rupture and compared clinical characteristics and angiographic findings between AMI and UA. Informed consent was obtained from all patients enrolled in this study.

Criteria of AMI and UA

UA was defined as either an exacerbation of angina that was previously stable, such as angina occurring at rest, or the new onset of chest pain occurring at rest. The diagnosis of AMI was based on a characteristic history of prolonged chest pain, diagnostic electrocardiographic changes, an elevation in the serum creatine kinase level, the creatine kinase MB fraction ($\geq$2 times the upper limit of the normal value), and/or elevation of troponin T levels ($\geq$0.1 ng/ml).

Coronary Angiography

Coronary angiography was performed with standard procedures from the femoral or radial arteries. After 2,000 units of heparin was administered, qualifying and quantitative angiography was performed to assess lesion morphology and the severity of stenosis. Each coronary artery was closely observed with at least two projections in the right coronary artery and three projections in the left anterior descending artery and left circumflex artery. Quantitative coronary angiograms were analyzed with a computer-assisted, automated edge-detection algorithm (CMS, Medical Imaging System, Nuenen, The Netherlands) by one angiographer. The qualitative morphologic analyses of all angiograms were performed by two experienced angiographers who were blinded to clinical presentation.

Evaluation of Ischemia- or Infarct -Related Arteries and Lesions

IRAs were defined as arteries originally perfusing an area distal to the lesion on a specific coronary artery on the basis of the distribution of transient or persistent ischemic ST-T changes on 12-lead electrocardiography, transient or persistent asynergic area on two-dimensional echocardiography, left ventriculography, and scintigraphy. After the locations of IRAs were determined, ischemia- or infarct-related lesions (IRLs) could be identified. IRLs were the most severe lesions or complex lesions in the IRAs.

Evaluation of Plaque Disruption Sites

We classified the coronary angiographic morphology of AMI and UA into six categories, which included total occlusion, simple lesions (type I), and four variable degrees of luminal narrowing (types IIa, IIb, IIc, IId)[6] **(Fig. 1)**. Type I lesions represent luminal narrowing resulting from negative endoluminal images with smooth borders and broad necks. Type IIa lesions represented irregular, poorly defined, or hazy borders with sharp leading or trailing edges that either overhung or were perpendicular to the vessel walls. Type IIb lesions, including ulcerative lesions, were characterized by focal external eversion or protrusion of contrast media and diffuse luminal irregularities. Type IIc lesions included luminal narrowing with ellipsoid contrast pooling adjacent to the diseased portion, i.e., so-called extraluminal contrast pooling, and single or

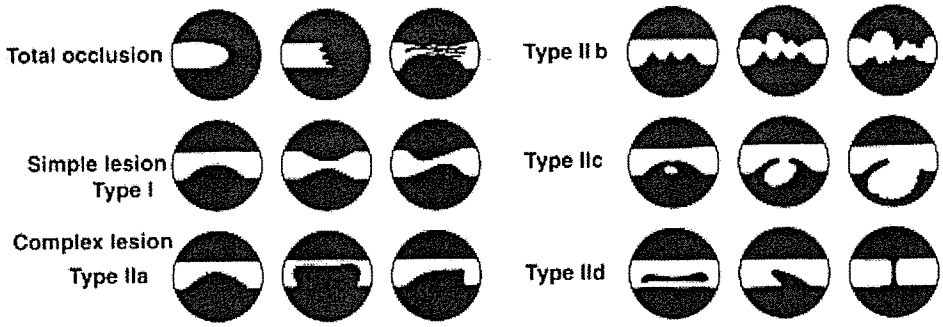

Fig. 1 Angiographical morphologies of plaque disruption site

paired short, thin, linear radiolucency with or without a variable degree of outpouching, and definite outpouching with or without radiolucency. Type IId lesions included variable forms and grades of linear or club-shaped intraluminal radiolucency caused by membranous or band-like structures. These radiolucent lesions may be parallel, spiraled, angulated, or perpendicular to the vessel wall. An angiographic plaque rupture was defined as an ulceration and an angle between the plaque shoulder and the vessel wall, for example a narrow neck.

According to the definition of IRLs, plaque rupture sites were divided into two groups, namely an upstream type and a downstream type. If the plaque rupture site was at the proximal portion of the maximum stenotic site, it was defined as an upstream type, and if the plaque rupture site was at the distal portion, it was defined as a downstream type. However, we could not determine the upstream or downstream part in cases of total occlusion, simple lesions, multiple ulcerations, or slit lesions or in cases with ulceration in the middle of stenosis.

Statistical Analysis

Data are expressed as the means ± SD. categorical variables were analyzed with the chi-square test or Fisher's exact provability test. Whether data were normally distributed or not was examined with the Kolmogrov-Sminov test. If data were normally distributed, an unpaired Student's *t*-test or Welch's *t*-test was used to compare groups. Otherwise, the Mann-Whitney U test was used. Differences were considered to be statistically significant at $p<0.05$.

Results

Plaque Disruption Site

Two hundred twenty patients, including 121 patients with simple lesions and 99 patients with total occlusion, were excluded from this study because plaque rupture sites could not be diagnosed. Forty-seven patients with complex lesions were also excluded because the upstream or downstream part of the plaque rupture could not be determined. Nine patients with small or thin anatomic coronary structures could not be evaluated with the coronary angiography equipment. Finally, 72 patients in whom the upstream or downstream plaque rupture sites could be clearly identified were included in this study.

Of the 72 patients with clearly identified plaque rupture sites, 45 had AMI and 27 had UA. In the AMI group, 27 sites were categorized upstream type and 18 as downstream. In the UA group, 5 sites were categorized as upstream and 22 as downstream. The frequency of upstream sites was significantly higher in patients with AMI than in those with UA. On the other hand, the frequency of downstream sites was higher in patients with UA than in those with AMI. Between the AMI group and the UA group, there were no significant differences in percent diameter stenosis, minimum lumen diameter, or lesion length (**Table 1**).

Cases of the upstream type and downstream types are shown in **Figure 2, 3**, respectively.

Baseline and Angiographic Characteristics

The baseline and angiographic characteristics of

Table 1 Lesion Characteristics on Angiogram

	Acute Myocardial Infarction n=45	Unstable Angina n=27	*P*
Disruption Site			
Upstream	27 (60.0)	5 (18.5)	<0.05
Downstream	18 (40.0)	22 (81.5)	
QCA Analysis			
Percent Diameter Stenosis, %	88±13	89±11	0.76
Minimal Lumen Diameter, mm	0.98±0.55	0.96±0.26	0.72
Lesion Length, mm	6.77±2.64	8.24±1.40	0.15

Values are n (%) or the mean±SD. QCA indicates quantitative coronary angiography.

Fig. 2 Plaque disruption at upstream site in patient with AMI

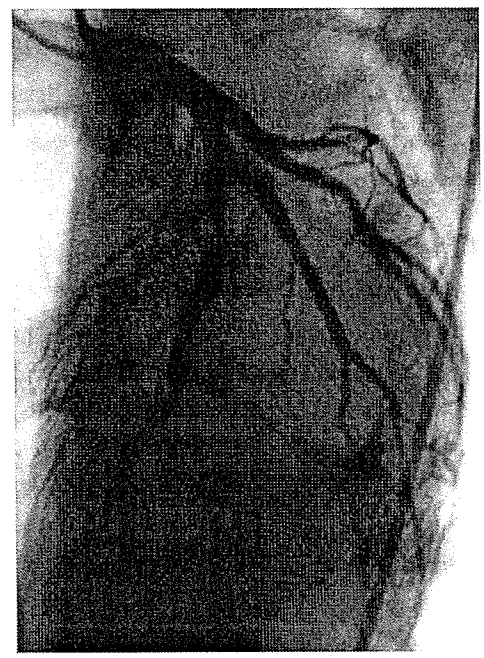

Fig. 3 Plaque disruption at downstream in patient with UA

the AMI group and the UA group are summarized in **Table 2**. There were no significant differences in age, gender, body mass index, plasma lipid levels, or the frequencies of diabetes mellitus, hypertension, or smoking habit. In addition, no significant differences were observed in the location of culprit coronary arteries or the number of diseased vessels.

Angiographic Morphology of Plaque Disruption Sites

There were no significant differences in the angiographic morphology of plaque rupture sites between the AMI and UA groups. However, type IIa lesions, which demonstrated irregular, poorly defined, or hazy borders with sharp leading or trailing edges that hung over the vessel walls, were a major morphological finding in each group. A type IIc lesion was observed in only one patient with UA, whereas type IId lesions were observed in 6 patients with AMI and in 9 patients with UA (**Table 3**).

Differentiation of Plaque Disruption Sites in Patients with AMI

The AMI group included 34 patients with ST elevation myocardial infarction and 11 patients with non-ST elevation myocardial infarction. There were no significant differences in plaque rupture sites between the groups (**Table 4**). There were no significant differences in other baseline characteristics between the groups.

Discussion

To the best of our knowledge, this is the first study to find that AMI arises from a plaque